

Speed limits on classical chaos

Swetamber Das^{1,2} and Jason R. Green^{1,2,*}

¹*Department of Chemistry, University of Massachusetts Boston, Boston, MA 02125*

²*Department of Physics, University of Massachusetts Boston, Boston, MA 02125*

Uncertainty in the initial conditions of dynamical systems can cause exponentially fast divergence of trajectories – a signature of deterministic chaos. Here, we show that local dynamical (in)stability sets a classical speed limit on the observables of classical systems. For systems with a time-invariant local stability matrix, this speed limit simplifies to a classical analog of the Mandelstam-Tamm time-energy uncertainty relation. These classical bounds derive from a Fisher information that we define in terms of Lyapunov vectors on tangent space, analogous to the quantum Fisher information defined in terms of wavevectors on Hilbert space. As in quantum dynamics, this information measure for the fluctuations in local stability of the state space sets an upper bound on the time of classical, dynamical systems to evolve between two states. The bounds it sets apply to systems that are open or closed, conservative or dissipative, driven or passive, and directly connects the geometries of phase space and information.

Quantum speed limits are fundamental constraints on the time evolution of quantum mechanical systems [1]. For example, Mandelstam and Tamm’s version of the time-energy uncertainty relation sets a speed limit on the observables of unitary quantum dynamics [2]. It has since been extended [3] to open quantum systems [4–7] and connected to parameter estimation [8–11], information theory [12–14], and many-body dynamics [15, 16]. These bounds quantify the inherent limitation on measurements of dynamical quantities in physical systems [17, 18]. It was recently discovered that there are bounds on the evolution of classical systems, the earliest of which largely rely on the Hilbert space of the Liouville equation [19, 20]. For a purely stochastic dynamics, there is now a growing number of thermodynamic speed limits [21–23] on the flux of energy and entropy between a system and external reservoirs. For example, there is a stochastic thermodynamic analog of the Mandelstam-Tamm bound [24], both of which can be expressed as time-information uncertainty relations, and combining these classical and quantum mechanical results gives a more general speed limit on the observables of open quantum systems [25]. However, because all the currently known classical speed limits are on statistical dynamics, an open challenge is setting speed limits on the underlying physical dynamics, dynamics that often exhibit deterministic chaos.

Deterministic chaos is signature of many classical dynamical systems evolving under a strongly nonlinear dynamics. Measuring chaos has given insights into the physical mechanisms of the jamming transition in granular materials [26], self-organizing systems [27], evaporating collections of nuclei, equilibrium and nonequilibrium fluids [28–30], and critical phenomena [31]. A characteristic of deterministic chaos is the divergence of initially close phase space trajectories [32], with the rates of diver-

gence setting an intrinsic timescale for the exploration of state space. This feature of dynamical systems, and the growing connections between dynamical systems theory and nonequilibrium statistical mechanics [32, 33], raise the question of whether there are classical speed limits on the intrinsic timescales of deterministic chaos.

In this Letter, we leverage the classical density matrix formulation of dynamical systems in Ref. 34 (and the generalization of Liouville’s equation there) to derive classical speed limits on observables that exactly parallel the Mandelstam-Tamm bound. We define a timescale as the time it takes the mean of a given observable to reach the value of one initial standard deviation. As in quantum mechanics, we derive two necessary ingredients for the classical time-information uncertainty relations that set speed limits on observables: the tangent space analogs of the Ehrenfest theorem and quantum Fisher information. Using these new results, we derive speed limits on the underlying dynamics of any classical system, be it open or closed, dissipative or conservative, passively evolving or actively driven.

Heuristic argument.— A speed limit on the convergence/divergence of classical trajectories requires, first, the identification of an intrinsic speed. Take two points, initially arbitrarily close, separated by a distance $\|\delta\mathbf{x}(t_0)\| = \|\mathbf{x}(t_0) - \mathbf{x}'(t_0)\|$. When the dynamics are sensitive to initial conditions, the distance grows to $\|\delta\mathbf{x}(t)\|$ at an intrinsic rate $r(t')$ over a time $\tau = t - t_0$; the largest Lyapunov exponent, λ , measures the exponential rate at which the distance between two trajectories diverges (or converges) in state space, $e^{\lambda\tau}$ [35]. With this Lyapunov exponent, a plausible speed limit would be the time for the distance to grow by e : $\|\delta\mathbf{x}(t)\|/\|\delta\mathbf{x}(t_0)\| \approx e$ or $\ln \|\delta\mathbf{x}(t)\| - \ln \|\delta\mathbf{x}(t_0)\| = \lambda\tau \geq 1$. Loosely speaking, the divergence of initially close trajectories would determine the timescale τ on which the behavior of the system is predictable and beyond which it is chaotic. The time it takes for the distance between two nearby phase points to

* jason.green@umb.edu

increase by exactly a factor of e , known as the Lyapunov time, τ_L , would saturate this heuristic bound $\lambda\tau_L \approx 1$.

To derive a speed limit more rigorously, and for other observables, we instead start from the linearized dynamics to derive an upper bound on the rates of tangent space observables, including the Lyapunov exponents.

Dynamics of the classical density matrix.— Consider a generic dynamical system $\dot{\mathbf{x}} = \mathbf{F}[\mathbf{x}(t)]$, where \mathbf{x} represents a point $\mathbf{x}(t) := [x^1(t), x^2(t), \dots, x^n(t)]^\top$ in an n -dimensional state space. Infinitesimal perturbations $|\delta\mathbf{x}(t)\rangle$ in the tangent space represent uncertainty about the initial condition; these vectors stretch, contract, and rotate over time under the linearized dynamics,

$$d_t |\delta\mathbf{x}(t)\rangle = \mathbf{A}[\mathbf{x}(t)] |\delta\mathbf{x}(t)\rangle, \quad (1)$$

with the stability matrix, $\mathbf{A} := \mathbf{A}[\mathbf{x}(t)] = \nabla\mathbf{F}$ having the elements $(\mathbf{A})_j^i = \partial\dot{x}^i(t)/\partial x^j(t)$. Dirac's notation here represents a finite-dimensional vector (its transpose) with the ket (bra): $|\delta\mathbf{x}(t)\rangle := [\delta x^1(t), \delta x^2(t), \dots, \delta x^n(t)]^\top \in T\mathcal{M}$. These linearized dynamics are an established approach to analyze the stability of nonlinear dynamical systems [35]. Solving the equation of motion,

$$|\delta\mathbf{x}(t)\rangle = \mathcal{T}_+ e^{\int_{t_0}^{t+t_0} \mathbf{A}(t') dt'} |\delta\mathbf{x}(t_0)\rangle, \quad (2)$$

gives the perturbation vector at a time t in terms of the propagator (with time ordering operator \mathcal{T}_+ because stability matrices at two different times do not generally commute). This evolution operator is reminiscent of the Dyson series and interaction picture in quantum mechanics [36]. However, unlike the quantum Hamiltonian (a Hermitian operator), the stability matrix is generally not symmetric and the tangent space evolution operator is generally not unitary.

Through our classical density matrix formulation [34], we can construct a norm-preserving operator for the tangent space dynamics of a *unit* perturbation vector. A normalized density matrix for a “pure” perturbation state describing a unit perturbation $|\delta\mathbf{u}(t)\rangle = |\delta\mathbf{x}(t)\rangle/\|\delta\mathbf{x}(t)\|$ is a projection operator, $\boldsymbol{\rho}(t) = |\delta\mathbf{u}(t)\rangle\langle\delta\mathbf{u}(t)|$, with the properties one expects of a pure state [34]. Its time evolution is governed by an equation of motion,

$$d_t \boldsymbol{\rho} = \{\mathbf{A}_+, \boldsymbol{\rho}\} + [\mathbf{A}_-, \boldsymbol{\rho}] - 2\langle\mathbf{A}_+\rangle\boldsymbol{\rho}, \quad (3)$$

akin to the von Neumann equation in quantum dynamics. Here, $\langle\mathbf{A}_+\rangle = \text{Tr}(\mathbf{A}_+\boldsymbol{\rho})$ and \mathbf{A}_\pm represent the symmetric and anti-symmetric parts of \mathbf{A} appearing in the anti-commutator $\{\cdot\}$ and the commutator $[\cdot]$, respectively. This norm-preserving dynamics holds regardless of whether the dynamical system is Hamiltonian or dissipative.

The symmetric part \mathbf{A}_+ determines the rate of stretching of tangent vectors. The expectation value $\langle\mathbf{A}_+\rangle$ is, in fact, the instantaneous Lyapunov exponent for the linearized dynamics, $r[\mathbf{x}(t)] = d_t \ln \|\delta\mathbf{u}(t)\|$. It is related to

the finite-time Lyapunov exponent:

$$\lambda(t, t_0) = |t|^{-1} \int_{t_0}^{t+t_0} r[\mathbf{x}(t')] dt'. \quad (4)$$

This classical density matrix formulation of dynamical systems leads to a generalization of Liouville's theorem and Liouville's equation [34]. In this framework, \mathbf{A}_+ is the matrix representation of an “observable” in tangent space.

In what follows, we focus on pure states (a single perturbation to the state variables of a classical system). However, our results also holds for *maximally* mixed normalized states, $\boldsymbol{\rho}'(t) = k^{-1} \sum_{i=1}^k \boldsymbol{\rho}_i(t)$, which also evolve according to Eq. 3. In this case, expectation values are to be computed with respect to $\boldsymbol{\rho}'$.

Tangent-space observables.— Motivated by formulations of quantum mechanics, we represent observables in the tangent space by $n \times n$ square matrices, \mathbf{O} . These are linear operators living in a real inner product space that evolve in time along a given trajectory in an n -dimensional state space.

Their expectation value with respect to the density matrix $\boldsymbol{\rho}$ is $\langle\mathbf{O}\rangle := \langle\mathbf{O}\rangle_{\boldsymbol{\rho}} = \langle\delta\mathbf{u}|\mathbf{O}|\delta\mathbf{u}\rangle = \text{Tr}(\mathbf{O}\boldsymbol{\rho})$. For instance, the instantaneous and finite-time Lyapunov exponents are:

$$r = \langle\mathbf{A}_+\rangle = \text{Tr}(\mathbf{A}_+\boldsymbol{\rho}), \quad \lambda(t, t_0) = \frac{1}{2t} \ln \text{Tr}(\boldsymbol{\xi}\boldsymbol{\rho}), \quad (5)$$

where $\boldsymbol{\xi} = |\delta\mathbf{x}(t)\rangle\langle\delta\mathbf{x}(t)|$. Geometrically, the mean of an observable $\langle\mathbf{O}\rangle = \text{Tr}(\mathbf{O}\boldsymbol{\rho})$ for a pure perturbation state is the scalar projection of $|\delta\mathbf{u}\rangle$ on $\mathbf{O}|\delta\mathbf{u}\rangle$.

For instance, the instantaneous Lyapunov exponent is the projection of $|\delta\mathbf{u}\rangle$ on $\mathbf{A}_+|\delta\mathbf{u}\rangle$. The mean $\langle\mathbf{A}_-\rangle = 0$, so the anti-symmetric matrix \mathbf{A}_- continuously projects $|\delta\mathbf{u}\rangle$ onto an orthogonal vector at each moment of time (i.e., \mathbf{A}_- rotates $|\delta\mathbf{u}\rangle$ by $\pi/2$).

From the dynamics of the state, we can derive the time evolution of the moments $\langle\mathbf{O}\rangle$ of any observable \mathbf{O} (Supplemental Material, SM I):

$$d_t \langle\mathbf{O}\rangle = \text{cov}(\mathbf{O}, 2\mathbf{A}^\top) + \langle d_t \mathbf{O} \rangle, \quad (6)$$

the tangent space analog of Ehrenfest's theorem (Heisenberg's equation) for quantum mechanical observables [37] with an additional anticommutator term. The covariance, $\text{cov}(\mathbf{X}, \mathbf{Y}) = \langle\mathbf{X}\mathbf{Y}^\top\rangle - \langle\mathbf{X}\rangle\langle\mathbf{Y}^\top\rangle$, is composed of two pieces: the mean anticommutator, $\text{cov}(\mathbf{O}, 2\mathbf{A}_+) = \langle\{\mathbf{O}, \mathbf{A}_+\}\rangle - 2\langle\mathbf{A}_+\rangle\langle\mathbf{O}\rangle$, and the mean commutator, $\text{cov}(\mathbf{O}, 2\mathbf{A}_-) = \langle[\mathbf{O}, \mathbf{A}_-]\rangle$. Both are symmetric matrices and themselves tangent space observables. The chosen basis determines the form of the equation of motion of the density matrix [34] and observables. If dynamics are Hamiltonian, the equation of motion can be expressed,

$$\{H, \langle\mathbf{O}\rangle\}_P = \text{cov}(\mathbf{O}, 2\mathbf{A}^\top) + \langle d_t \mathbf{O} \rangle, \quad (7)$$

in terms of the Hamiltonian of the system H and the Poisson bracket $\{\cdot\}_P$. Equation 6 is also similar in mathematical form to the equation of motion for stochastic thermodynamic observables [24] and Price's equation in population biology [38]. Another distinction here is that the

commutator term comes with the *anti*-symmetric part \mathbf{A}_- of the stability matrix, unlike the mean commutator in the Ehrenfest theorem which is made up of Hermitian operators. Furthermore, if the observables \mathbf{O} and $\boldsymbol{\rho}$ commute (i.e., if they share the same set of eigenbasis), the covariance term vanishes: $\text{cov}(\mathbf{O}, 2\mathbf{A}^\top) = 0$ and Eq. 6 reduces to $d_t\langle\mathbf{O}\rangle = \langle d_t\mathbf{O}\rangle$, a result which also holds for quantum mechanical observables (SM II).

With the equation of motion for moments of observables, we can derive classical uncertainty relations that set limits on the speed at which they evolve. To derive these bounds, we first define a tangent space Fisher information analogous to the quantum Fisher information.

Tangent-space Fisher information.— Whether classical or quantum mechanical, the Fisher information is a fundamental ingredient in optimal measurements, setting a lower bound on the variance of unbiased estimators of parameters through the Cramér-Rao information inequality. It is also an intrinsic speed on the evolution of a system between neighboring states [39, 40] Geometrically, the Fisher information matrix is a Riemannian metric on a quantum statistical manifold [11].

The norm-preserving dynamics of the classical density matrix allows us to define a Fisher information (matrix) on the tangent space. Re-writing the equation of motion for the density matrix from Eq. 3,

$$d_t\boldsymbol{\rho} = \bar{\mathbf{A}}\boldsymbol{\rho} + \boldsymbol{\rho}\bar{\mathbf{A}}^\top, \quad (8)$$

in terms of the deviation $\bar{\mathbf{A}} = \mathbf{A} - \langle\mathbf{A}\rangle$ defines a logarithmic derivative \mathbf{L} implicitly through $d_t\boldsymbol{\rho} := \frac{1}{2}(\boldsymbol{\rho}\mathbf{L} + \mathbf{L}^\top\boldsymbol{\rho})$ [41, 42], SM III. Using \mathbf{L} , the equation of motion for an observable \mathbf{O} in Eq. 6 is: $d_t\langle\mathbf{O}\rangle = \text{cov}(\mathbf{O}, \mathbf{L}) + \langle d_t\mathbf{O}\rangle$. The total logarithmic derivative $\mathbf{L} = 2\mathbf{A}^\top = 2(\mathbf{A}^\top - \langle\mathbf{A}\rangle)$ has a mean $\langle\mathbf{L}\rangle = 0$. We define the tangent-space Fisher information for pure states in a basis-independent form,

$$\mathcal{I}_F = \Delta\mathbf{L}^2 = \langle\mathbf{L}\mathbf{L}^\top\rangle = 4(\Delta\mathbf{A}^\top)^2, \quad (9)$$

as the expectation value of the Fisher information matrix $\mathbf{L}\mathbf{L}^\top$, the variance of the total logarithmic derivative. For pure states, the Fisher information here is the variance in local stability $(\Delta\mathbf{A}^\top)^2 = \langle\mathbf{A}^\top\mathbf{A}\rangle - \langle\mathbf{A}_+\rangle^2$, just as the quantum Fisher information is the variance in the energy $\tilde{\mathcal{I}}_F = 4\Delta\hat{\mathcal{H}}^2/\hbar^2$ for pure quantum states evolving under a unitary dynamics.

In quantum estimation theory, \mathbf{L} is a symmetric operator [11, 43]. By contrast, our choice of the (total) logarithmic derivative here is dictated by Eq. 8. However, it can be partitioned into its symmetric and antisymmetric parts,

$$\mathbf{L}_+ = 2(\mathbf{A}_+ - \langle\mathbf{A}_+\rangle) \quad \text{and} \quad \mathbf{L}_- = -2\mathbf{A}_-, \quad (10)$$

with mean $\langle\mathbf{L}_\pm\rangle = 0$ and variance $\Delta\mathbf{L}_\pm^2 = \langle\mathbf{L}_\pm^2\rangle$.

As a consequence, the Fisher information partitions into three components:

$$\mathcal{I}_F = \mathcal{I}_+ + \mathcal{I}_- + \langle\mathbf{L}_C\rangle. \quad (11)$$

The symmetric and antisymmetric parts are also variances $\mathcal{I}_\pm = \langle\mathbf{L}_\pm^2\rangle = 4\Delta\mathbf{A}_\pm^2$. The third term is the commutator of logarithmic derivatives, $\mathbf{L}_C = [\mathbf{L}_-, \mathbf{L}_+] = 4[\mathbf{A}_+, \mathbf{A}_-]$, a traceless symmetric matrix. (SM V includes a geometrical interpretation.)

The term $\langle\mathbf{L}_C\rangle$, is a covariance: $\langle\mathbf{L}_C\rangle = 4\text{cov}(\mathbf{A}_-, \mathbf{A}_+)$. This *mixed* term follows the cosine law and is related to angle between vectors $\mathbf{L}_+|\delta\mathbf{u}\rangle$ and $\mathbf{L}_-|\delta\mathbf{u}\rangle$, SM IV.

Time-information uncertainty relations.—

With the preceding groundwork, we can derive speed limits on time-evolving tangent space observables for classical, deterministic dynamical systems, including those determining the degree of classical chaos. To see this, we solve Eq. 6:

$$\dot{\mathcal{O}} := \text{cov}(\mathbf{O}, \mathbf{L}) = d_t\langle\mathbf{O}\rangle - \langle d_t\mathbf{O}\rangle. \quad (12)$$

A dynamical measure of the variation in \mathbf{O} is defined by the time it takes for the magnitude of this path function $\mathcal{O} = \int \dot{\mathcal{O}}dt$ to have the value of one standard deviation $\Delta\mathbf{O}$. If $\dot{\mathcal{O}}$ is constant, this time $\tau_{\mathcal{O}}$ is approximately:

$$|\mathcal{O}| = \left| \int_{t_0}^{t_0+\tau_{\mathcal{O}}} \dot{\mathcal{O}}dt \right| \approx |\dot{\mathcal{O}}|\tau_{\mathcal{O}} \approx \Delta\mathbf{O}. \quad (13)$$

As in quantum mechanics [25, 37] and stochastic thermodynamics [24, 44], we define an intrinsic speed for the time evolution of \mathbf{O} :

$$\frac{1}{\tau_{\mathcal{O}}} := \frac{|\dot{\mathcal{O}}|}{\Delta\mathbf{O}} = \frac{|\text{cov}(\mathbf{O}, \mathbf{L})|}{\Delta\mathbf{O}}. \quad (14)$$

In quantum mechanics, the observable $\hat{\mathcal{Q}}$, the mean commutator $\langle[\hat{\mathcal{Q}}, \hat{\mathbf{H}}]\rangle$ takes the role of the covariance term in Eq. 14 and the term $\langle d_t\hat{\mathcal{Q}}\rangle$ in the Ehrenfest equation vanishes. But, in the case of a generic classical dynamical system, $\langle d_t\mathbf{O}\rangle$ does not necessarily vanish. This term is nonzero for many dynamical systems, as it is common for the stability matrix to be time dependent.

Applying Cauchy-Schwartz inequality to the covariance gives a classical uncertainty relation:

$$\text{cov}(\mathbf{O}, \mathbf{L})^2 \leq \Delta\mathbf{O}^2 \Delta\mathbf{L}^2. \quad (15)$$

Using the tangent-space Fisher information, this upper bound immediately leads to the following time-information uncertainty relation:

$$\tau_{\mathcal{O}}\sqrt{\mathcal{I}_F} \geq 1 \quad \text{or} \quad \tau_{\mathcal{O}}\Delta\mathbf{A}^\top \geq \frac{1}{2}. \quad (16)$$

The tangent space Fisher information as the intrinsic speed $\mathcal{I}_F = \tau^{-1}$ that sets the limit on the speed $\tau_{\mathcal{O}}^{-1}$ of any observable. This global speed limit is further divisible into speed limits on the symmetric and antisymmetric parts of the stability matrix. Splitting the covariance term, $\text{cov}(\mathbf{O}, \mathbf{L}) = \text{cov}(\mathbf{O}, \mathbf{L}_+) + \text{cov}(\mathbf{O}, \mathbf{L}_-)$, we identify two timescales: $\tau_{\mathcal{O}, \pm}^{-1} := |\text{cov}(\mathbf{O}, \mathbf{L}_\pm)|/\Delta\mathbf{O}$. This partitioning decouples the influence of the symmetric and

anti-symmetric parts of the stability matrix on the evolution of the observable, operating on separate time scales $\tau_{\mathcal{O},+}$ and $\tau_{\mathcal{O},-}$. These timescales also have speed limits, again through the Cauchy-Schwartz inequality, as:

$$\tau_{\mathcal{O},\pm} \sqrt{\mathcal{I}_{\pm}} \geq 1. \quad (17)$$

The Fisher information contributions \mathcal{I}_{\pm} are related to the stretching/contraction and rotation of the vector $|\delta\mathbf{u}\rangle$ (SM IV). The former \mathcal{I}_+ is fixed by the instantaneous Lyapunov exponent and its magnitude sets the maximum threshold on, for example, the rate of stretching of a tangent vector. The inequalities above are then speed limits on the development of chaos in any dynamical system.

Applying the triangle inequality to the covariance, $\text{cov}(\mathbf{O}, \mathbf{L})$, we can find upper and lower speed limits on the timescale of the observable: $|\tau_{\mathcal{O},+}^{-1} - \tau_{\mathcal{O},-}^{-1}| \leq \tau_{\mathcal{O}}^{-1} \leq \tau_{\mathcal{O},+}^{-1} + \tau_{\mathcal{O},-}^{-1}$.

Combining this with Eq. 11, we find that the geometric mean of \mathcal{I}_{\pm} sets an upper bound on $|\langle \mathbf{L}_C \rangle|$ (SM V):

$$|\langle \mathbf{L}_C \rangle| \leq 2\sqrt{\mathcal{I}_+ \mathcal{I}_-}. \quad (18)$$

Unlike the other subordinate bounds, this speed limit is specific to the evolution of the system through state space. We have thus found a family of uncertainty relations wherein the Fisher information (and its constituents) upper bound the timescales governing the evolution of tangent space observables.

These speed limits in Eqs. 16 and 17 saturate for \mathbf{A}^{\top} and \mathbf{A}_{\pm} , respectively. In these cases, covariances simply reduce to variances (and half of the associated Fisher information):

$$\frac{1}{\tau} = \sqrt{\mathcal{I}_F} = 2\Delta\mathbf{A}^{\top}, \quad \frac{1}{\tau_{\pm}} = \sqrt{\mathcal{I}_{\pm}} = 2\Delta\mathbf{A}_{\pm}. \quad (19)$$

Saturation of the bounds occurs when the observable \mathbf{O} (\mathbf{O}_{\pm}) is linearly related to the logarithmic derivative \mathbf{L} (\mathbf{L}_{\pm}). SM VI shows saturation of the bounds for \mathbf{A}_- , \mathbf{A}^{\top} , and \mathbf{A} along a chaotic orbit in the Lorenz model.

In the absence of any explicit time dependence in \mathbf{O} , the second term in Eq. 6 vanishes, $d_t\langle\mathbf{O}\rangle = \text{cov}(\mathbf{O}, \mathbf{L})$. (A similar restriction on stochastic thermodynamic observables simplifies a more general bound [24] for time-independent observables to bounds based on the Cramér-Rao inequality [22, 23].) Applying the Cauchy-Schwartz inequality, as before, gives,

$$d_t\langle\mathbf{O}\rangle \leq \Delta\mathbf{O}\Delta\mathbf{L} = \Delta\mathbf{O}\sqrt{\mathcal{I}_F} = 2\Delta\mathbf{O}\Delta\mathbf{A}^{\top}, \quad (20)$$

the classical, tangent-space analog of the Mandelstam-Tamm uncertainty relation in quantum mechanics and the Cramér-Rao bound in classical statistics. Despite these striking similarities, this bound holds for the comparatively few dynamical systems where \mathbf{A} is time independent; two examples are the harmonic oscillator and the model for Chua's circuit [45]. Most nonlinear systems actually violate this bound, requiring the more general

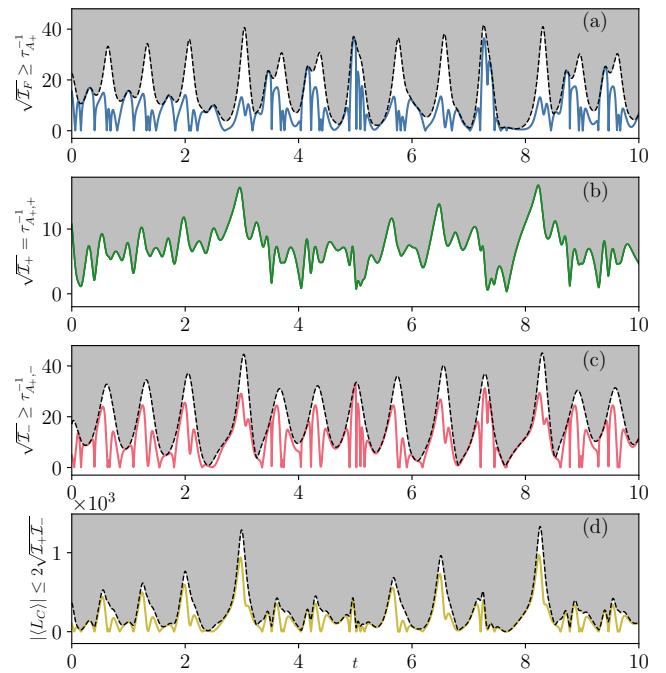


Figure 1. *Speed limit on chaos: the instantaneous Lyapunov exponent, $r(t) = \langle \mathbf{A}_+ \rangle$, for a chaotic orbit of the Lorenz model.*— (a) Square root of the tangent-space Fisher information (dashed black) $\sqrt{\mathcal{I}_F}$ upper bounds the speed $\tau_{\mathbf{A}_+}^{-1}$ (solid blue). (b) For this observable, the speed $\tau_{\mathbf{A}_{+,+}}^{-1}$ saturates the bound set by $\sqrt{\mathcal{I}_+}$ (solid green). (c) The speed $\tau_{\mathbf{A}_{+,-}}^{-1}$ (solid red) is bounded by $\sqrt{\mathcal{I}_-}$ (dashed black). (d) The mixed term $|\langle \mathbf{L}_C \rangle|$ (solid yellow) is bounded by $2\sqrt{\mathcal{I}_+ \mathcal{I}_-}$ (dashed black) from above. Shaded regions mark speeds not accessible to the observable. The parameters of the Lorenz model are: $\sigma = 10$, $\beta = 8/3$, $\rho = 28$.

bound, Eq. 16. However, the uncertainty relation for deterministic systems in Eq. 16 holds universally, regardless of the nature of dynamics.

Returning to our heuristic argument, we choose the instantaneous Lyapunov exponent, $r(t) := \langle \mathbf{A}_+ \rangle$ as an observable to numerically confirm the validity of Eqs. 16 and 17 for a sample chaotic orbit of the Lorenz model. Figure 1(a) shows the time evolution of the tangent space Fisher information (see Eq. 9) setting the upper limit on the speed of $\langle \mathbf{A}_+ \rangle$ (computed from Eq. 14). For \mathbf{A}_+ , $\tau_{\mathcal{O},+}^{-1}$ saturates the bound $\sqrt{\mathcal{I}_+}$ (Fig. 1(b)). The piece $\sqrt{\mathcal{I}_-}$ bounds the speed $\tau_{\mathbf{A}_{+,-}}^{-1}$ in Fig. 1(c) while the mixed term satisfies the inequality in Eq. 18 shown in Fig. 1(d). The SM includes more examples of bounds on the speed of observables: the Lorenz model in SM VIIA and the Hénon-Heiles system in SM VIIB.

Conclusions.— It is well known that uncertainty in the initial conditions of dynamical systems devolves into chaotic behavior with characteristic timescales set by the Lyapunov exponents. Here, we showed that for a broad class of dynamical systems, this uncertainty and the sensitivity to initial conditions must obey (time-

information) uncertainty relations. These classical uncertainty relations are speed limits on the evolution of tangent space observables, including the instantaneous Lyapunov exponents whose time average are often studied phase space invariants. These speed limits derive from a classical density matrix formulation of deterministic dynamical systems that has parallels with quantum mechanics, suggesting possibilities for further cross-pollination of theories. For example, by defining observables in the tangent space, we derived their equation of motion, which is similar to Ehrenfest's theorem. Among these observables, it is the Fisher information for deter-

ministic dynamical systems that appears in all of these time-information uncertainty relations, setting the classical speed limit, and partitioning into symmetric and anti-symmetric parts that set subordinate speed limit on classical observables. All of these speed limits on observables are model independent and therefore applicable to arbitrary deterministic systems.

Acknowledgments.— This material is based upon work supported by the National Science Foundation under Grant No. 2124510 and 1856250. This publication was also made possible, in part, through the support of a grant from the John Templeton Foundation.

-
- [1] S. Deffner and S. Campbell, Quantum speed limits: From Heisenberg's uncertainty principle to optimal quantum control, *J. Phys. A* **50**, 453001 (2017).
- [2] L. Mandelstam and I. Tamm, The uncertainty relation between energy and time in non-relativistic quantum mechanics, in *Selected Papers*, edited by I. E. Tamm, B. M. Bolotovskii, V. Y. Frenkel, and R. Peierls (Springer, Berlin, Heidelberg, 1991) pp. 115–123.
- [3] P. Busch, The time–energy uncertainty relation, in *Time in Quantum Mechanics*, Lecture Notes in Physics, edited by J. Muga, R. S. Mayato, and Í. Egusquiza (Springer, Berlin, Heidelberg, 2008) pp. 73–105.
- [4] M. M. Taddei, B. M. Escher, L. Davidovich, and R. L. de Matos Filho, Quantum speed limit for physical processes, *Phys. Rev. Lett.* **110**, 050402 (2013).
- [5] A. del Campo, I. L. Egusquiza, M. B. Plenio, and S. F. Huelga, Quantum speed limits in open system dynamics, *Phys. Rev. Lett.* **110**, 050403 (2013).
- [6] S. Deffner and E. Lutz, Quantum speed limit for non-Markovian dynamics, *Phys. Rev. Lett.* **111**, 010402 (2013).
- [7] L. P. García-Pintos and A. del Campo, Quantum speed limits under continuous quantum measurements, *New J. Phys.* **21**, 033012 (2019).
- [8] S. L. Braunstein, C. M. Caves, and G. J. Milburn, Generalized uncertainty relations: Theory, examples, and Lorentz invariance, *Ann. Phys.* **247**, 135 (1996).
- [9] V. Giovannetti, S. Lloyd, and L. Maccone, Advances in quantum metrology, *Nature Photon* **5**, 222 (2011).
- [10] M. Beau and A. del Campo, Nonlinear quantum metrology of many-body open systems, *Phys. Rev. Lett.* **119**, 010403 (2017).
- [11] J. S. Sidhu and P. Kok, Geometric perspective on quantum parameter estimation, *AVS Quantum Sci.* **2**, 014701 (2020).
- [12] J. Jing, L.-A. Wu, and A. del Campo, Fundamental speed limits to the generation of quantumness, *Sci. Rep.* **6**, 38149 (2016).
- [13] S. Deffner, Quantum speed limits and the maximal rate of information production, *Phys. Rev. Research* **2**, 013161 (2020).
- [14] D. P. Pires, K. Modi, and L. C. Céleri, Bounding generalized relative entropies: Nonasymptotic quantum speed limits, *Phys. Rev. E* **103**, 032105 (2021).
- [15] T. Fogarty, S. Deffner, T. Busch, and S. Campbell, Orthogonality catastrophe as a consequence of the quantum speed limit, *Phys. Rev. Lett.* **124**, 110601 (2020).
- [16] A. del Campo, Probing quantum speed limits with ultracold gases, *Phys. Rev. Lett.* **126**, 180603 (2021).
- [17] N. Margolus and L. B. Levitin, The maximum speed of dynamical evolution, *Physica D* **120**, 188 (1998).
- [18] S. Lloyd, Ultimate physical limits to computation, *Nature* **406**, 1047 (2000).
- [19] B. Shanahan, A. Chenu, N. Margolus, and A. del Campo, Quantum speed limits across the quantum-to-classical transition, *Phys. Rev. Lett.* **120**, 070401 (2018).
- [20] M. Okuyama and M. Ohzeki, Quantum speed limit is not quantum, *Phys. Rev. Lett.* **120**, 070402 (2018).
- [21] N. Shiraishi, K. Funo, and K. Saito, Speed limit for classical stochastic processes, *Phys. Rev. Lett.* **121**, 070601 (2018).
- [22] Y. Hasegawa and T. Van Vu, Uncertainty relations in stochastic processes: An information inequality approach, *Phys. Rev. E* **99**, 062126 (2019).
- [23] S. Ito and A. Dechant, Stochastic time evolution, information geometry, and the Cramér-Rao bound, *Phys. Rev. X* **10**, 021056 (2020).
- [24] S. B. Nicholson, L. P. García-Pintos, A. del Campo, and J. R. Green, Time–information uncertainty relations in thermodynamics, *Nat. Phys.* **16**, 1211 (2020).
- [25] L. P. García-Pintos, S. B. Nicholson, J. R. Green, A. del Campo, and A. V. Gorshkov, Unifying quantum and classical speed limits on observables, *ArXiv:2108.04261 Cond-Mat Physicsquant-Ph* (2021), [arXiv:2108.04261 \[cond-mat, physics-quant-ph\]](https://arxiv.org/abs/2108.04261).
- [26] E. J. Banigan, M. K. Illich, D. J. Stace-Naughton, and D. A. Egolf, The chaotic dynamics of jamming, *Nat. Phys.* **9**, 288 (2013).
- [27] J. R. Green, A. B. Costa, B. A. Grzybowski, and I. Szleifer, Relationship between dynamical entropy and energy dissipation far from thermodynamic equilibrium, *Proc. Natl. Acad. Sci. U.S.A.* **110**, 16339 (2013).
- [28] D. J. Evans and G. P. Morriss, *Statistical Mechanics of Nonequilibrium Liquids* (ANU Press).
- [29] H. Bosetti and H. A. Posch, What does dynamical systems theory teach us about fluids?, *Commun. Theor. Phys.* **62**, 451 (2014).
- [30] M. Das and J. R. Green, Self-averaging fluctuations in the chaoticity of simple fluids, *Phys. Rev. Lett.* **119**, 115502 (2017).
- [31] M. Das and J. R. Green, Critical fluctuations and slowing down of chaos, *Nat. Commun.* **10**, 2155 (2019).

- [32] P. Gaspard, *Chaos, Scattering and Statistical Mechanics*, Cambridge Nonlinear Science Series (Cambridge University Press, Cambridge, 1998).
- [33] J. R. Dorfman, *An Introduction to Chaos in Nonequilibrium Statistical Mechanics*, Cambridge Lecture Notes in Physics (Cambridge University Press, Cambridge, 1999).
- [34] S. Das and J. R. Green, Density matrix formulation of dynamical systems, ArXiv210605911 Cond-Mat Physic-snlin (2021), [arXiv:2106.05911 \[cond-mat, physics:nlin\]](#).
- [35] A. Pikovsky and A. Politi, *Lyapunov Exponents: A Tool to Explore Complex Dynamics* (Cambridge University Press, Cambridge, 2016).
- [36] C. J. Joachain, *Quantum Collision Theory* (North-Holland, 1983).
- [37] A. Messiah, *Quantum Mechanics* (Dover Publications, 1999).
- [38] G. R. Price, Selection and covariance, *Nature* **227**, 520 (1970).
- [39] E.-j. Kim, U. Lee, J. Heseltine, and R. Hollerbach, Geometric structure and geodesic in a solvable model of nonequilibrium process, *Phys. Rev. E* **93**, 062127 (2016).
- [40] S. W. Flynn, H. C. Zhao, and J. R. Green, Measuring disorder in irreversible decay processes, *J. Chem. Phys.* **141**, 104107 (2014); J. W. Nichols, S. W. Flynn, and J. R. Green, Order and disorder in irreversible decay processes, *J. Chem. Phys.* **142**, 064113 (2015).
- [41] A. Fujiwara and H. Nagaoka, Quantum Fisher metric and estimation for pure state models, *Phys. Lett. A* **201**, 119 (1995).
- [42] M. Tsang, H. M. Wiseman, and C. M. Caves, Fundamental quantum limit to waveform estimation, *Phys. Rev. Lett.* **106**, 090401 (2011).
- [43] M. G. A. Paris, Quantum estimation for quantum technology, *Int. J. Quantum Inform.* **07**, 125 (2009).
- [44] S. B. Nicholson and J. R. Green, Thermodynamic speed limits from the regression of information, ArXiv210501588 Cond-Mat (2021), [arXiv:2105.01588 \[cond-mat\]](#).
- [45] L. O. Chua, Chua's circuit 10 years later, *Int. J. Circuit Theory Appl.* **22**, 279 (1994).

Supplemental Material: Speed limits on classical chaos

Swetamber Das^{1,2} and Jason R. Green^{1,2,*}

¹*Department of Chemistry, University of Massachusetts Boston, Boston, MA 02125*

²*Department of Physics, University of Massachusetts Boston, Boston, MA 02125*

I. EQUATION OF MOTION OF THE MEAN OF AN OBSERVABLE

The mean of an arbitrary observable represented by a symmetric matrix \mathbf{O} for a general pure state $\boldsymbol{\rho}$ is written as $\langle \mathbf{O} \rangle = \text{Tr}(\boldsymbol{\rho} \mathbf{O})$. Its time derivative is given by

$$\begin{aligned} d_t \langle \mathbf{O} \rangle &= \text{Tr}(\mathbf{O} d_t \boldsymbol{\rho}) + \text{Tr}(\boldsymbol{\rho} d_t \mathbf{O}) \\ &= \text{Tr}(\mathbf{O} \{ \mathbf{A}_+, \boldsymbol{\rho} \}) + \text{Tr}(\mathbf{O} [\mathbf{A}_-, \boldsymbol{\rho}]) - 2 \langle \mathbf{A}_+ \rangle \text{Tr}(\boldsymbol{\rho} \mathbf{O}) \\ &\quad + \text{Tr}(\boldsymbol{\rho} d_t \mathbf{O}) \\ &= 2(\langle \mathbf{O} \mathbf{A}_+ \rangle - \langle \mathbf{O} \rangle \langle \mathbf{A}_+ \rangle) + \langle [\mathbf{O}, \mathbf{A}_-] \rangle + \langle d_t \mathbf{O} \rangle \\ &= \text{cov}(\mathbf{O}, 2\mathbf{A}_+) - \text{cov}(\mathbf{O}, 2\mathbf{A}_-) + \langle d_t \mathbf{O} \rangle, \\ &= \text{cov}(\mathbf{O}, 2\mathbf{A}^\top) + \langle d_t \mathbf{O} \rangle. \end{aligned} \quad (21)$$

where $\text{cov}(\mathbf{X}, \mathbf{Y}) = \langle \mathbf{X} \mathbf{Y}^\top \rangle - \langle \mathbf{X} \rangle \langle \mathbf{Y}^\top \rangle$. We have also used the following relations: $\langle \{ \mathbf{O}, \mathbf{A}_- \} \rangle = 0$ and $\langle \mathbf{A}_- \rangle = 0$.

For example, the time-derivative of the ILE is given by

$$\dot{r} = d_t \langle \mathbf{A}_+ \rangle = 2\Delta \mathbf{A}_+^2 + 2 \langle \mathbf{A}_+ \mathbf{A}_- \rangle + \langle d_t \mathbf{A}_+ \rangle.$$

For Hamiltonian dynamics, we can represent the relation using Poisson bracket $\{ \cdot \}_P$ as follows,

$$\{ r, H \}_P = 2\Delta \mathbf{A}_+^2 + 2 \langle \mathbf{A}_+ \mathbf{A}_- \rangle + \langle d_t \mathbf{A}_+ \rangle.$$

II. THE EHRENFEST THEOREM IN DENSITY MATRIX BASIS

Consider the time evolution equation of a mean observable $\langle \mathbf{O} \rangle$ (Eq. 21). If the observable \mathbf{O} and $\boldsymbol{\rho}$ commute, then they share the same set of eigenbasis. We then have

$$\mathbf{O} \boldsymbol{\rho} = \boldsymbol{\rho} \mathbf{O} = \mathbf{O} |\delta \mathbf{u}\rangle \langle \delta \mathbf{u}| = \alpha \boldsymbol{\rho},$$

where α is an eigenvalue of \mathbf{O} .

Thus, the covariance term in Eq. 21 becomes:

$$\begin{aligned} \text{cov}(\mathbf{O}, 2\mathbf{A}^\top) &= 2 \langle \mathbf{O} \mathbf{A} \rangle - 2 \langle \mathbf{O} \rangle \langle \mathbf{A} \rangle \\ &= 2 \text{Tr}(\mathbf{O} \mathbf{A} \boldsymbol{\rho}) - 2 \text{Tr}(\mathbf{O} \boldsymbol{\rho}) \text{Tr}(\mathbf{A} \boldsymbol{\rho}) \\ &= 2 \text{Tr}(\boldsymbol{\rho} \mathbf{O} \mathbf{A}) - 2 \text{Tr}(\mathbf{O} \boldsymbol{\rho}) \text{Tr}(\mathbf{A} \boldsymbol{\rho}) \\ &= 2\alpha \text{Tr}(\mathbf{A} \boldsymbol{\rho}) - 2\alpha \text{Tr}(\mathbf{A} \boldsymbol{\rho}) = 0. \end{aligned}$$

This reduces Eq. 21 to

$$d_t \langle \mathbf{O} \rangle = \langle d_t \mathbf{O} \rangle.$$

III. PURE STATES

Consider the equation of motion for $\boldsymbol{\rho}$:

$$d_t \boldsymbol{\rho} = \bar{\mathbf{A}} \boldsymbol{\rho} + \boldsymbol{\rho} \bar{\mathbf{A}}^\top.$$

We multiply $\boldsymbol{\rho}$ from the left and right to write the following two equations:

$$\boldsymbol{\rho} (d_t \boldsymbol{\rho}) = \boldsymbol{\rho} \bar{\mathbf{A}} \boldsymbol{\rho} + \boldsymbol{\rho}^2 \bar{\mathbf{A}}^\top, \quad \text{and} \quad (d_t \boldsymbol{\rho}) \boldsymbol{\rho} = \bar{\mathbf{A}} \boldsymbol{\rho}^2 + \boldsymbol{\rho} \bar{\mathbf{A}}^\top \boldsymbol{\rho}.$$

Adding these equations,

$$d_t(\boldsymbol{\rho}^2) = \bar{\mathbf{A}} \boldsymbol{\rho}^2 + \boldsymbol{\rho}^2 \bar{\mathbf{A}}^\top, \quad (22)$$

where we have used $\boldsymbol{\rho} \bar{\mathbf{A}} \boldsymbol{\rho} = \boldsymbol{\rho} \bar{\mathbf{A}}^\top \boldsymbol{\rho} = 0$.

The RHS of Eq. 22 becomes $d_t \boldsymbol{\rho}$ iff $\boldsymbol{\rho}^2 = \boldsymbol{\rho}$.

IV. FISHER INFORMATION

The symmetric and anti-symmetric parts of the stability matrix contributes to the Fisher information as follows (see the main text):

$$\mathcal{I}_\pm = \langle \mathbf{L}_\pm^2 \rangle = 4\Delta \mathbf{A}_\pm^2.$$

For a pure perturbation state, these quantities are given by:

$$\begin{aligned} \Delta \mathbf{A}_+^2 &= \langle \mathbf{A}_+^2 \rangle - \langle \mathbf{A}_+ \rangle^2 \\ &= \langle \delta \mathbf{u} | \mathbf{A}_+ \mathbf{A}_+ | \delta \mathbf{u} \rangle - \langle \delta \mathbf{u} | \mathbf{A}_+ | \delta \mathbf{u} \rangle^2 \\ &= \|\mathbf{A}_+ | \delta \mathbf{u} \rangle\|^2 - \cos^2 \alpha \|\mathbf{A}_+ | \delta \mathbf{u} \rangle\|^2 \\ &= (1 - \cos^2 \alpha) \|\mathbf{A}_+ | \delta \mathbf{u} \rangle\|^2 = \sin^2 \alpha \|\mathbf{A}_+ | \delta \mathbf{u} \rangle\|^2, \end{aligned}$$

* jason.green@umb.edu

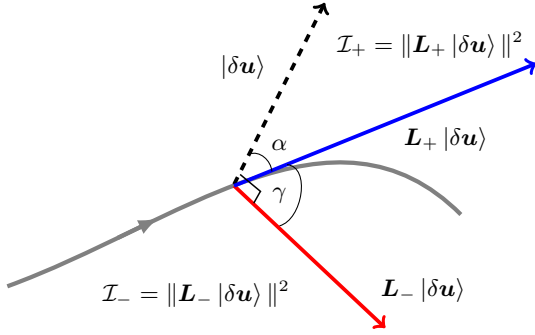


Figure SM1. A perturbation vector $|\delta\mathbf{u}\rangle$ on a given trajectory in phase space. The vector $\mathbf{A}_+|\delta\mathbf{u}\rangle$ makes an angle α with $|\delta\mathbf{u}\rangle$ and the vector $\mathbf{L}_-|\delta\mathbf{u}\rangle$ is orthogonal to $|\delta\mathbf{u}\rangle$. The Fisher information contributors \mathcal{I}_\pm are given by the magnitudes of these vectors as shown.

where α is the angle between the vectors $|\delta\mathbf{u}\rangle$ and $\mathbf{L}_+|\delta\mathbf{u}\rangle$ given by $\cos\alpha = \frac{\langle\delta\mathbf{u}|\mathbf{L}_+|\delta\mathbf{u}\rangle}{\|\mathbf{L}_+|\delta\mathbf{u}\rangle\|}$. Next, we have

$$\Delta\mathbf{A}_-^2 = \langle\mathbf{A}_-^2\rangle = \langle\delta\mathbf{u}|\mathbf{A}_-\mathbf{A}_-^\top|\delta\mathbf{u}\rangle = \|\mathbf{A}_-|\delta\mathbf{u}\rangle\|^2.$$

The resulting vector $\mathbf{A}_-|\delta\mathbf{u}\rangle$ is perpendicular to $|\delta\mathbf{u}\rangle$:

$$\langle\delta\mathbf{u}|\mathbf{A}_-|\delta\mathbf{u}\rangle = \text{Tr}(\mathbf{A}_-\boldsymbol{\rho}) = 0,$$

as the trace of the product of a symmetric and an anti-symmetric matrices vanishes.

Finally, these two Fisher information contributors are,

$$\begin{aligned}\mathcal{I}_+ &= \|\mathbf{L}_+|\delta\mathbf{u}\rangle\|^2 = 4\sin^2\alpha\|\mathbf{A}_+|\delta\mathbf{u}\rangle\|^2, \\ \mathcal{I}_- &= \|\mathbf{L}_-|\delta\mathbf{u}\rangle\|^2 = 4\|\mathbf{A}_-|\delta\mathbf{u}\rangle\|^2.\end{aligned}$$

See Fig. SM1 for a pictorial depiction of this geometric interpretation.

Next, consider the *mixed* term $\mathbf{L}_C = 4[\mathbf{A}_+, \mathbf{A}_-]$. Its expectation value can be expressed in several ways:

$$\begin{aligned}\langle\mathbf{L}_C\rangle &= \langle[\mathbf{A}_+, \mathbf{A}_-]\rangle = 8\text{cov}(\mathbf{A}_+, \mathbf{A}_-) \\ &= 2(\Delta\mathbf{A}^{\top 2} - \Delta\mathbf{A}^2) = 4(\Delta\mathbf{A}_+^2 + \Delta\mathbf{A}_-^2 - \Delta\mathbf{A}^2).\end{aligned}$$

It then follows the cosine law for vectors $\mathbf{L}^\top|\delta\mathbf{u}\rangle$ and $\mathbf{L}_\pm|\delta\mathbf{u}\rangle$ – if γ is the angle between the latter two vectors (Fig. SM1), we get

$$\langle\mathbf{L}_C\rangle = 8\Delta\mathbf{A}_+\Delta\mathbf{A}_-\cos\gamma.$$

V. BOUND ON L_C

Consider mean $\langle\mathbf{L}_C\rangle$:

$$\langle\mathbf{L}_C\rangle = 4\langle[\mathbf{A}_+, \mathbf{A}_-]\rangle = 8\text{cov}(\mathbf{A}_+, \mathbf{A}_-).$$

Using the Cauchy-Schwarz inequality, we get

$$8|\text{cov}(\mathbf{A}_+, \mathbf{A}_-)| = |\langle\mathbf{L}_C\rangle| \leq 8\Delta\mathbf{A}_+\Delta\mathbf{A}_- = 2\sqrt{\mathcal{I}_+}\sqrt{\mathcal{I}_-}.$$

So we get the following series of inequality:

$$|\langle\mathbf{L}_C\rangle| \leq 2\sqrt{\mathcal{I}_+\mathcal{I}_-}.$$

VI. SATURATION OF BOUNDS

- (a) $\tau_{\mathcal{O}}\sqrt{\mathcal{I}_F} \geq 1$: Choosing the observable to be \mathbf{A}^\top , we get

$$\begin{aligned}\tau_{\mathbf{A}^\top}^{-1} &= \frac{|\text{cov}(\mathbf{A}^\top, \mathbf{L})|}{\Delta\mathbf{O}} = \frac{|\text{cov}(\mathbf{A}^\top, 2\mathbf{A}^\top)|}{\Delta\mathbf{A}^\top} \\ &= 2\Delta\mathbf{A}^\top = \sqrt{\mathcal{I}_F}.\end{aligned}$$

- (b) $\tau_{\mathcal{O},\pm}\sqrt{\mathcal{I}_\pm} \geq 1$: Choosing the observable to be \mathbf{A}_\pm , we get

$$\begin{aligned}\tau_{\mathbf{A}_\pm,\pm}^{-1} &= \frac{|\text{cov}(\mathbf{A}_\pm, \mathbf{L})|}{\Delta\mathbf{O}} = \frac{|\text{cov}(\mathbf{A}_\pm, 2\mathbf{A}^\top)|}{\Delta\mathbf{A}^\top} \\ &= 2\Delta\mathbf{A}_\pm = \sqrt{\mathcal{I}_\pm}.\end{aligned}$$

VII. SPEED LIMITS ON SOME OBSERVABLES

A. The Lorenz model

We consider the model of atmospheric convection due to Lorenz and Fetter¹. The model is defined by the following set of ordinary differential equations,

$$\begin{aligned}\dot{x} &= \sigma(y - x) \\ \dot{y} &= x(\rho - z) - y \\ \dot{z} &= xy - \beta z,\end{aligned}$$

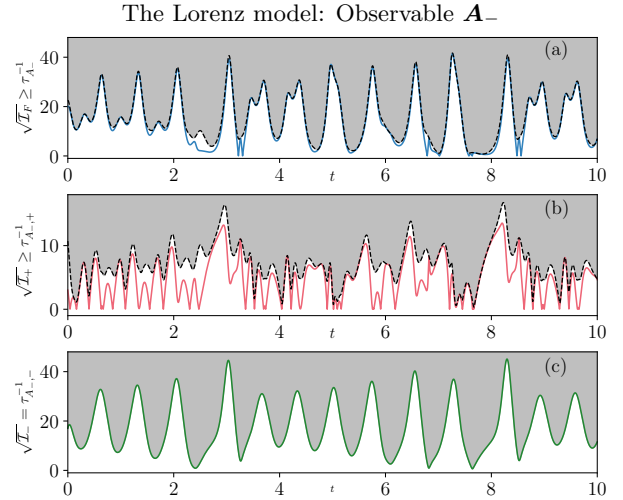


Figure SM2. The mean observable $\langle\mathbf{A}_-\rangle$, for a chaotic orbit of the Lorenz model.— (a) Square root of the tangent-space Fisher information (dashed black) $\sqrt{\mathcal{I}_F}$ upper bounds the speed $\tau_{\mathbf{A}_+}^{-1}$ (solid blue). (b) The speed $\tau_{\mathbf{A}_+,-}$ (solid red) is bounded by $\sqrt{\mathcal{I}_-}$ (dashed black). (c) For this observable, the speed $\tau_{\mathbf{A}_+,-}^{-1}$ saturates the bound set by $\sqrt{\mathcal{I}_+}$ (solid green). Shaded regions mark speeds not accessible to the observable.

¹ E. N. Lorenz, Deterministic nonperiodic flow, J. Atmospheric Sci. 20, 130 (1963).

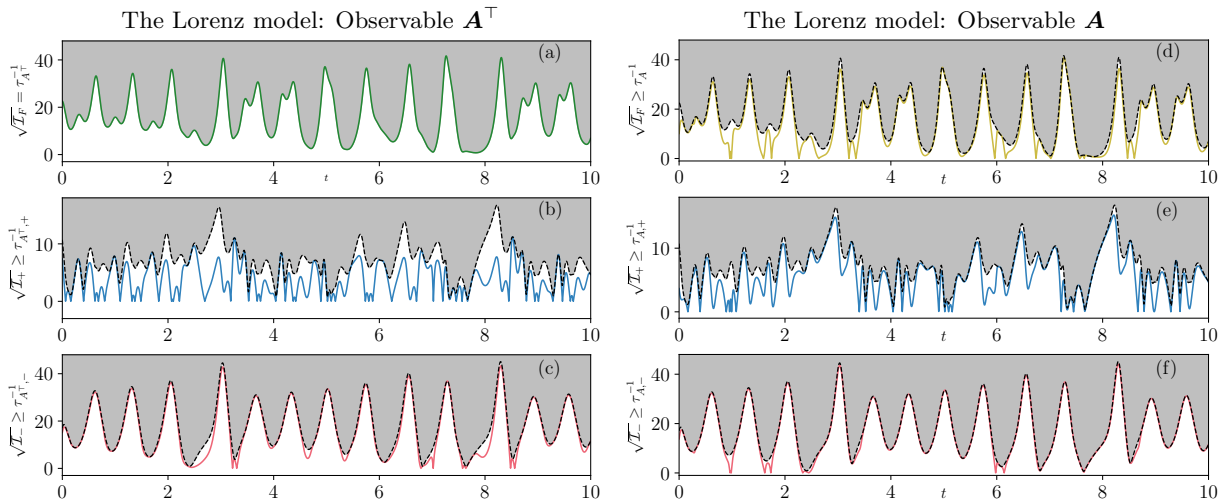


Figure SM3. Mean observables $\langle \mathbf{A}^\top \rangle$ and $\langle \mathbf{A} \rangle$, for a chaotic orbit of the Lorenz model.— (a) the speed $\tau_{\mathbf{A}^\top}^{-1}$ (solid green) saturates the square root of the tangent-space Fisher information (dashed black) $\sqrt{\mathcal{I}_F}$; $\sqrt{\mathcal{I}_+}$ (dashed black) upper bounds the speeds (solid blue) $\tau_{\mathbf{A}^\top,+}^{-1}$ in (b) and $\tau_{\mathbf{A},+}^{-1}$ in (e); $\sqrt{\mathcal{I}_-}$ (dashed black) upper bounds the speeds (solid blue) $\tau_{\mathbf{A}^\top,-}^{-1}$ in (c) and $\tau_{\mathbf{A},-}^{-1}$ in (f); $\sqrt{\mathcal{I}_F}$ upper bounds $\tau_{\mathbf{A}^\top}^{-1}$ in (b). Shaded regions mark speeds not accessible to the observable.

with the stability matrix:

$$\mathbf{A} = \begin{pmatrix} -\sigma & \sigma & 0 \\ \rho - z & -1 & -x \\ y & x & -\beta \end{pmatrix}.$$

Speed limits on mean observables \mathbf{A}_- , \mathbf{A}^\top and \mathbf{A} for a chaotic orbit of the Lorenz model (parameters: $\sigma = 10$, $\beta = 8/3$, $\rho = 28$) are plotted in Figs. SM2 and SM3.

B. The Hénon-Heiles system

We consider the Hénon-Heiles model² to numerically verify the speed limits obtained in the main text. It system is given by the following system of equations,

$$\begin{aligned} \dot{x} &= p_x, & \dot{y} &= p_y, \\ \dot{p}_x &= -x - 2xy, & \dot{p}_y &= -y - x^2 + y^2, \end{aligned}$$

which lead to the stability matrix:

$$\mathcal{H} = \begin{pmatrix} 0 & 0 & 1 & 0 \\ 0 & 0 & 0 & 1 \\ -1 - 2y & -2x & 0 & 0 \\ -2x & -1 + 2y & 0 & 0 \end{pmatrix}.$$

For a chaotic orbit of the system corresponding to energy $E = 0.1666$, we obtain plots in Figs. SM4 and SM5 for bounds on speed of mean observables \mathbf{A}_\pm , \mathbf{A}^\top and \mathbf{A} .

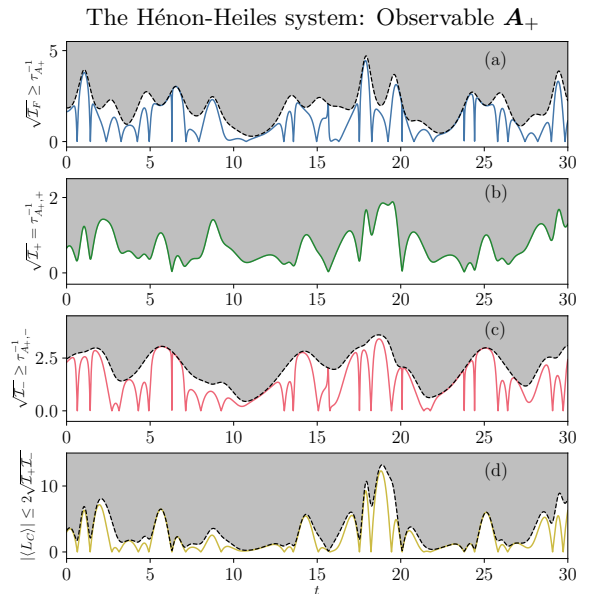


Figure SM4. Speed limit on chaos: the instantaneous Lyapunov exponent, $\langle \mathbf{A}_+ \rangle$, for a chaotic orbit of the Hénon-Heiles system.— (a) Square root of the tangent-space Fisher information (dashed black) $\sqrt{\mathcal{I}_F}$ upper bounds the speed $\tau_{\mathbf{A}_+}^{-1}$ (solid blue). (b) For this observable, the speed $\tau_{\mathbf{A}_+,+}^{-1}$ saturates the bound set by $\sqrt{\mathcal{I}_+}$ (solid green). (c) The speed $\tau_{\mathbf{A}_+,-}^{-1}$ (solid red) is bounded by $\sqrt{\mathcal{I}_-}$ (dashed black). (d) The mixed term $|\langle \mathbf{L}_C \rangle|$ (solid yellow) is bounded by $2\sqrt{\mathcal{I}_+\mathcal{I}_-}$ (dashed black) from above. Shaded regions mark speeds not accessible to the observable.

² M. Hénon and C. Heiles, The applicability of the third integral of motion: Some numerical experiments, Astron. J. 69, 73 (1964).

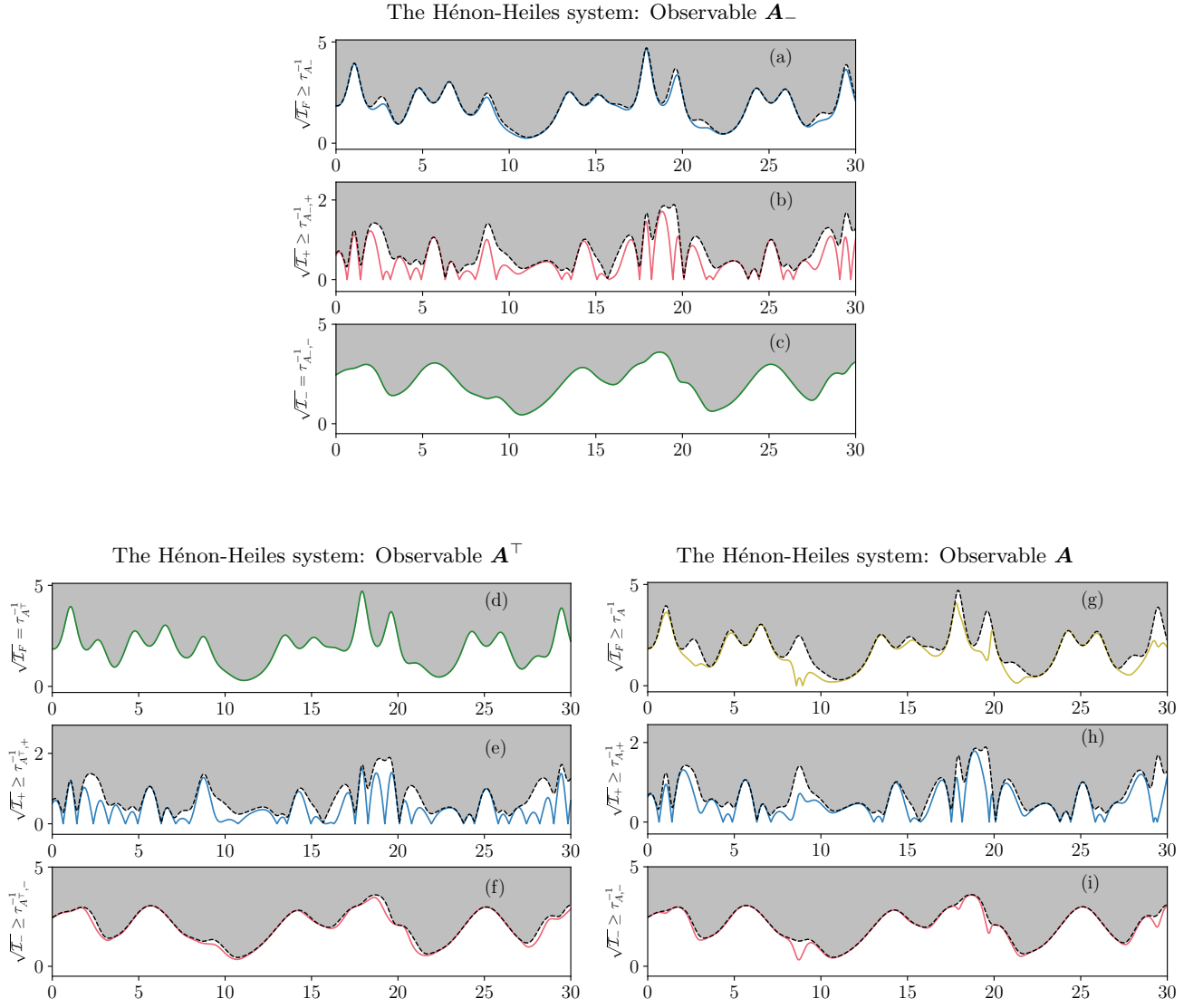


Figure SM5. Mean observables $\langle \mathbf{A}_- \rangle$, $\langle \mathbf{A}^\top \rangle$, and $\langle \mathbf{A} \rangle$, for a chaotic orbit of the Hénon-Heiles system.— Bounding curves indicating Fisher information and its pieces are in dashed black. (a) Observable \mathbf{A}_- speed $\tau_{\mathbf{A}_-}^{-1}$ (solid blue) is bounded by $\sqrt{\mathcal{I}_F}$. (b) The speed $\tau_{\mathbf{A}_-,+}^{-1}$ (solid red) is bounded by $\sqrt{\mathcal{I}_+}$. (c) The speed $\tau_{\mathbf{A}_-, -}^{-1}$ (solid green) saturates the bound $\sqrt{\mathcal{I}_-}$. (d) Observable speed $\tau_{\mathbf{A}^\top}^{-1}$ (solid green) saturates the bound $\sqrt{\mathcal{I}_F}$. (e) The speed $\tau_{\mathbf{A}^\top, +}^{-1}$ (solid blue) is bounded by $\sqrt{\mathcal{I}_+}$. (f) The speed $\tau_{\mathbf{A}^\top, -}^{-1}$ (solid red) is bounded by $\sqrt{\mathcal{I}_-}$. (g) Observable speed $\tau_{\mathbf{A}}^{-1}$ (solid yellow) is bounded by $\sqrt{\mathcal{I}_F}$. (h) The speed $\tau_{\mathbf{A}, +}^{-1}$ (solid blue) is bounded by $\sqrt{\mathcal{I}_+}$. (i) The speed $\tau_{\mathbf{A}, -}^{-1}$ (solid red) is bounded by $\sqrt{\mathcal{I}_-}$. Shaded regions mark speeds not accessible to the observable.